

UWThPh-1997-30  
HEPHY-PUB 671/97  
TGU-21  
TU-526  
hep-ph/9710286

# SUSY-QCD corrections to stop and sbottom decays into $W^\pm$ and $Z^0$ bosons

A. BARTL<sup>1</sup>, H. EBERL<sup>2</sup>, K. HIDAKA<sup>3</sup>,  
S. KRAML<sup>2</sup>, W. MAJEROTTO<sup>2</sup>, W. POROD<sup>1</sup>, Y. YAMADA<sup>4</sup>

(1) *Institut für Theoretische Physik, Universität Wien, A-1090 Vienna, Austria*  
(2) *Institut für Hochenergiephysik, Österreichische Akademie der Wissenschaften,  
A-1050 Vienna, Austria*  
(3) *Department of Physics, Tokyo Gakugei University, Koganei, Tokyo 184, Japan*  
(4) *Department of Physics, Tohoku University, Sendai 980-77, Japan*

## Abstract

We calculate the supersymmetric  $\mathcal{O}(\alpha_s)$  QCD corrections to stop and sbottom decays into vector bosons within the Minimal Supersymmetric Standard Model. We give analytic formulae and perform a numerical analysis of these decays. We find that SUSY-QCD corrections to the decay widths are typically  $-5\%$  to  $-10\%$  depending on the squark masses, squark mixing angles, and the gluino mass.

# 1 Introduction

In the Minimal Supersymmetric Standard Model (MSSM) [1] every quark has two scalar partners, the squarks  $\tilde{q}_L$  and  $\tilde{q}_R$ . In general  $\tilde{q}_L$  and  $\tilde{q}_R$  mix to form mass eigenstates  $\tilde{q}_1$  and  $\tilde{q}_2$  (with  $m_{\tilde{q}_1} < m_{\tilde{q}_2}$ ), the size of the mixing being proportional to the mass of the corresponding quark  $q$  [2]. Therefore, the scalar partners of the top quark (stops) are expected to be strongly mixed so that one mass eigenstate  $\tilde{t}_1$  can be rather light and the other one  $\tilde{t}_2$  heavy. The sbottoms  $\tilde{b}_L$  and  $\tilde{b}_R$  may also considerably mix for large  $\tan\beta = v_2/v_1$  (where  $v_1$  and  $v_2$  are the vacuum expectation values of the two Higgs doublets).

Squark pair production in  $e^+e^-$  annihilation including mixing has been studied at tree-level in Ref. [3], then including conventional QCD corrections in [4, 5], and supersymmetric (SUSY) QCD corrections in Ref. [6, 7]. The cross section of squark production at hadron colliders (LHC and Tevatron) in next-to-leading order of SUSY–QCD was given in Ref. [8].

While, quite naturally, most studies concentrated on  $\tilde{t}_1$  ( $\tilde{b}_1$ ) production and decays, those of the heavier  $\tilde{t}_2$  ( $\tilde{b}_2$ ) have been discussed much less [9, 10, 11]. These particles could be produced at the LHC or an  $e^+e^-$  Linear Collider. The decay patterns of the heavier mass eigenstates  $\tilde{t}_2$  ( $\tilde{b}_2$ ) can be very complex due to the many possible open decay channels. There are the decays ( $i, j = 1, 2; k = 1 \dots 4$ ):

$$\tilde{t}_i \rightarrow t \tilde{\chi}_k^0, b \tilde{\chi}_j^+, \quad \tilde{b}_i \rightarrow b \tilde{\chi}_k^0, t \tilde{\chi}_j^-, \quad (1)$$

and in case the mass splitting is large enough:

$$\begin{aligned} \tilde{t}_i &\rightarrow \tilde{b}_j W^+, & \tilde{b}_i &\rightarrow \tilde{t}_j W^-, \\ \tilde{t}_2 &\rightarrow \tilde{t}_1 Z^0, & \tilde{b}_2 &\rightarrow \tilde{b}_1 Z^0, \end{aligned} \quad (2)$$

and

$$\begin{aligned} \tilde{t}_i &\rightarrow \tilde{b}_j H^+, & \tilde{b}_i &\rightarrow \tilde{t}_j H^-, \\ \tilde{t}_2 &\rightarrow \tilde{t}_1 (h^0, H^0, A^0), & \tilde{b}_2 &\rightarrow \tilde{b}_1 (h^0, H^0, A^0). \end{aligned} \quad (3)$$

Stops and sbottoms can also decay strongly through  $\tilde{t}_i \rightarrow t \tilde{g}$  and  $\tilde{b}_i \rightarrow b \tilde{g}$ . If these decays are kinematically possible, they are important. The SUSY–QCD corrections to squark decays into charginos and neutralinos have been calculated in [12]. The SUSY–QCD corrections to squark decays into Higgs bosons have been treated in [13], and those into gluino in [14]. The decays to photon and gluon,  $\tilde{q}_2 \rightarrow \tilde{q}_1 \gamma$ ,  $\tilde{q}_1 g$ , which are absent at tree-level, are not induced by  $\mathcal{O}(\alpha_s)$  SUSY–QCD corrections either. This is due to  $SU(3)_c \times U(1)_{\text{em}}$  gauge invariance.

In this paper we calculate the  $\mathcal{O}(\alpha_s)$  SUSY–QCD corrections to the squark decays into  $W^\pm$  and  $Z^0$  bosons of eq. (2). The stop decays into vector bosons can be dominant in the parameter

region where (i)  $m_t (A_t - \mu \cot \beta)$ , appearing in the mass matrix, is large enough to give the necessary mass splitting, (ii)  $M$  and  $|\mu|$  are relatively large to suppress the decay modes to chargino, neutralino, and gluino, and (iii) the decays into Higgs particles are not so important (for instance,  $m_A$  is large). For sbottoms to decay into vector bosons instead of (i) it is necessary that  $m_b (A_b - \mu \tan \beta)$  is large enough to lead to a large mass splitting of  $\tilde{b}_1$  and  $\tilde{b}_2$ .

In calculating the SUSY–QCD corrections we work in the on-shell renormalization scheme and use dimensional reduction [15], which preserves supersymmetry at least at two–loop level. The gluon loop corrections are calculated in the Feynman gauge. The couplings of the squarks to vector bosons depend on the squark mixing angles for which an appropriate renormalization procedure is necessary. Here we use the renormalization prescription as introduced in [7], where it was applied to the case of  $e^+e^- \rightarrow \tilde{q}_i \bar{\tilde{q}}_j$ .

## 2 Tree–level formulae and notation

The current eigenstates  $\tilde{q}_L$  and  $\tilde{q}_R$  are related to their mass eigenstates  $\tilde{q}_1$  and  $\tilde{q}_2$  by

$$\begin{pmatrix} \tilde{q}_1 \\ \tilde{q}_2 \end{pmatrix} = \mathcal{R}^{\tilde{q}} \begin{pmatrix} \tilde{q}_L \\ \tilde{q}_R \end{pmatrix}, \quad \mathcal{R}^{\tilde{q}} = \begin{pmatrix} \cos \theta_{\tilde{q}} & \sin \theta_{\tilde{q}} \\ -\sin \theta_{\tilde{q}} & \cos \theta_{\tilde{q}} \end{pmatrix} \quad (0 \leq \theta_{\tilde{q}} < \pi). \quad (4)$$

In the  $(\tilde{q}_1, \tilde{q}_2)$  basis the squark interactions with  $Z^0$  and  $W^\pm$  bosons are given by:

$$\begin{aligned} \mathcal{L} = & -\frac{ig}{\cos \theta_W} Z_\mu (\mathcal{R}_{i1}^{\tilde{q}} \mathcal{R}_{j1}^{\tilde{q}} C_L + \mathcal{R}_{i2}^{\tilde{q}} \mathcal{R}_{j2}^{\tilde{q}} C_R) \tilde{q}_j^\dagger \overset{\leftrightarrow}{\partial}^\mu \tilde{q}_i \\ & -\frac{ig}{\sqrt{2}} \mathcal{R}_{i1}^{\tilde{t}} \mathcal{R}_{j1}^{\tilde{b}} W_\mu^- \tilde{b}_j^\dagger \overset{\leftrightarrow}{\partial}^\mu \tilde{t}_i - \frac{ig}{\sqrt{2}} \mathcal{R}_{i1}^{\tilde{b}} \mathcal{R}_{j1}^{\tilde{t}} W_\mu^+ \tilde{t}_j^\dagger \overset{\leftrightarrow}{\partial}^\mu \tilde{b}_i, \end{aligned} \quad (5)$$

where  $C_{L,R} = I_{3L,R}^q - e_q \sin^2 \theta_W$  with  $I_3^q$  the third component of the weak isospin and  $e_q$  the electric charge. Here it is assumed that the  $(3,3)$  element of the super–CKM matrix  $\tilde{K}_{33} = 1$ .

At tree–level the amplitude of a squark decay into a  $W^\pm$  or  $Z^0$  boson has the general form

$$\mathcal{M}_0(\tilde{q}_i^\alpha \rightarrow \tilde{q}_j^\beta V) = -ig c_{ijV} (k_1 + k_2)^\mu \epsilon_\mu^*(k_3), \quad (6)$$

with  $k_1$ ,  $k_2$ , and  $k_3$  the four–momenta of  $\tilde{q}_i^\alpha$ ,  $\tilde{q}_j^\beta$ , and the vector boson  $V$  ( $V = W^\pm, Z^0$ ), respectively (Fig. 1a).  $\alpha$  and  $\beta$  are flavor indices. In the following we define  $m_i = m_{\tilde{q}_i^\alpha}$ ,  $m_j = m_{\tilde{q}_j^\beta}$ ,  $\mathcal{R}_{ik} = \mathcal{R}_{ik}^{\tilde{q}^\alpha}$ ,  $\mathcal{R}_{jk} = \mathcal{R}_{jk}^{\tilde{q}^\beta}$  for simplicity. Moreover, we shall use primes to explicitly distinguish between different flavors.

With this notation the  $\tilde{q}_i^\alpha$ - $\tilde{q}_j^\beta$ - $V$  couplings  $c_{ijV}$  are:

$$\begin{aligned} c_{ijZ} &= \frac{1}{\cos \theta_W} (\mathcal{R}_{i1} \mathcal{R}_{j1} C_L + \mathcal{R}_{i2} \mathcal{R}_{j2} C_R) \\ &= \frac{1}{\cos \theta_W} \begin{pmatrix} I_{3L}^q \cos^2 \theta_{\tilde{q}} - e_q \sin^2 \theta_W & -\frac{1}{2} I_{3L}^q \sin 2\theta_{\tilde{q}} \\ -\frac{1}{2} I_{3L}^q \sin 2\theta_{\tilde{q}} & I_{3L}^q \sin^2 \theta_{\tilde{q}} - e_q \sin^2 \theta_W \end{pmatrix}_{ij}, \end{aligned} \quad (7)$$

$$c_{ijW} = \frac{1}{\sqrt{2}} \mathcal{R}_{i1} \mathcal{R}'_{j1} = \frac{1}{\sqrt{2}} \begin{pmatrix} \cos \theta_{\tilde{q}} \cos \theta_{\tilde{q}'} & -\cos \theta_{\tilde{q}} \sin \theta_{\tilde{q}'} \\ -\sin \theta_{\tilde{q}} \cos \theta_{\tilde{q}'} & \sin \theta_{\tilde{q}} \sin \theta_{\tilde{q}'} \end{pmatrix}_{ij}. \quad (8)$$

The tree-level decay width can thus be written as [9]

$$\Gamma^0(\tilde{q}_i^\alpha \rightarrow \tilde{q}_j^\beta V) = \frac{g^2 (c_{ijV})^2 \kappa^3(m_i^2, m_j^2, m_V^2)}{16\pi m_V^2 m_i^3}, \quad (9)$$

with  $\kappa(x, y, z) = (x^2 + y^2 + z^2 - 2xy - 2xz - 2yz)^{1/2}$ .

Note that the decay  $\tilde{q}_{L(R)} \rightarrow \tilde{q}_{R(L)} Z^0$  does not occur at tree-level, and  $\tilde{q}_i \rightarrow \tilde{q}'_j W^\pm$  is not allowed at tree-level if one of the squarks is a pure “right” state.

### 3 SUSY–QCD corrections

The  $\mathcal{O}(\alpha_s)$  loop corrected decay amplitude is obtained by the shift:

$$c_{ijV} \rightarrow c_{ijV} + \delta c_{ijV}^{(v)} + \delta c_{ijV}^{(w)} + \delta c_{ijV}^{(c)}, \quad (10)$$

in eq. (6). The superscript  $v$  denotes the vertex correction (Figs. 1 b–f),  $w$  the wave function correction (Figs. 1 g–i), and  $c$  the counterterm to the couplings. Thus the  $\mathcal{O}(\alpha_s)$  corrected decay width  $\Gamma$  is given by

$$\Gamma = \Gamma^0 + \delta\Gamma^{(v)} + \delta\Gamma^{(w)} + \delta\Gamma^{(c)} + \delta\Gamma_{real} \quad (11)$$

where

$$\delta\Gamma^{(a)} = \frac{g^2 \kappa^3(m_i^2, m_j^2, m_V^2)}{8\pi m_V^2 m_i^3} c_{ijV} \operatorname{Re} \left\{ \delta c_{ijV}^{(a)} \right\} \quad (a = v, w, c). \quad (12)$$

$\delta\Gamma_{real}$  is the correction due to real gluon emission (Figs. 1j–l) which is included in order to cancel the infrared divergence. The total correction can be decomposed into a gluon (exchange and emission) contribution  $\delta\Gamma^{(g)}$ , and a gluino–exchange contribution  $\delta\Gamma^{(\tilde{g})}$ :  $\Gamma = \Gamma^0 + \delta\Gamma^{(g)} + \delta\Gamma^{(\tilde{g})}$ . The contribution from squark loops (Figs. 1f,i) cancels out in our renormalization scheme.

### 3.1 Vertex corrections

The vertex corrections stem from the five diagrams shown in Figs. 1 b–f. The gluon–exchange graphs of Figs. 1b–d yield

$$\begin{aligned} \delta c_{ijV}^{(v,g)} = & -\frac{\alpha_s}{3\pi} c_{ijV} \left[ B_0(m_i^2, \lambda^2, m_i^2) + B_0(m_j^2, \lambda^2, m_j^2) \right. \\ & \left. - 2(m_i^2 + m_j^2 - m_W^2)(C_0 + C_1 + C_2) \right]. \end{aligned} \quad (13)$$

$B_0$  and  $C_{0,1,2}$  are the standard two– and three–point functions [16] for which we follow the conventions of [17]. Here we use the abbreviation  $C_m = C_m(m_i^2, m_V^2, m_j^2; \lambda^2, m_i^2, m_j^2)$ . A gluon mass  $\lambda$  is introduced to regularize the infrared divergence.

The gluino–exchange contribution, Fig. 1e, gives

$$\begin{aligned} \delta c_{21Z}^{(v,\tilde{g})} = & -\frac{\alpha_s}{3\pi \cos \theta_W} \left\{ I_{3L}^q [2m_{\tilde{g}}^2 C_0 + m_{\tilde{q}_2}^2 C_1 + m_{\tilde{q}_1}^2 C_2 + (m_{\tilde{g}}^2 - m_q^2)(C_1 + C_2) + B_0] \sin 2\theta_{\tilde{q}} \right. \\ & \left. + 2m_{\tilde{g}} m_q (I_{3L}^q - 2e_q \sin^2 \theta_W) (C_0 + C_1 + C_2) \cos 2\theta_{\tilde{q}} \right\}, \end{aligned} \quad (14)$$

with  $C_m = C_m(m_{\tilde{q}_2}^2, m_Z^2, m_{\tilde{q}_1}^2; m_{\tilde{g}}^2, m_q^2, m_q^2)$  and  $B_0 = B_0(m_Z^2, m_q^2, m_q^2)$ , for the decay  $\tilde{q}_2 \rightarrow \tilde{q}_1 Z^0$ , and

$$\begin{aligned} \delta c_{ijW}^{(v,\tilde{g})} = & -\frac{\sqrt{2}}{3} \frac{\alpha_s}{\pi} \left\{ m_{\tilde{g}} (C_0 + C_1 + C_2) (m_q \mathcal{R}_{i2} \mathcal{R}'_{j1} + m_{q'} \mathcal{R}_{i1} \mathcal{R}'_{j2}) \right. \\ & - [m_i^2 C_1 + m_j^2 C_2 + m_{\tilde{g}}^2 (2C_0 + C_1 + C_2) + B_0] \mathcal{R}_{i1} \mathcal{R}'_{j1} \\ & \left. - m_q m_{q'} (C_1 + C_2) \mathcal{R}_{i2} \mathcal{R}'_{j2} \right\} \end{aligned} \quad (15)$$

with  $C_m = C_m(m_i^2, m_W^2, m_j^2; m_{\tilde{g}}^2, m_q^2, m_{q'}^2)$  and  $B_0 = B_0(m_W^2, m_q^2, m_{q'}^2)$ , for the decay  $\tilde{q}_i \rightarrow \tilde{q}'_j W^\pm$ . The squark loop of Fig. 1f does not contribute because it is proportional to the four–momentum of the vector boson. The total vertex correction is thus given by:

$$\delta c_{ijV}^{(v)} = \delta c_{ijV}^{(v,g)} + \delta c_{ijV}^{(v,\tilde{g})}. \quad (16)$$

### 3.2 Wave–function correction

The wave–function correction is given by

$$\delta c_{ijV}^{(w)} = \frac{1}{2} \left[ \delta \tilde{Z}_{ii}(\tilde{q}_i^\alpha) + \delta \tilde{Z}_{jj}(\tilde{q}_j^\beta) \right] c_{ijV} + \delta \tilde{Z}_{ik}(\tilde{q}_i^\alpha) c_{kjV} + \delta \tilde{Z}_{jl}(\tilde{q}_j^\beta) c_{ilV}, \quad (i \neq k, j \neq l). \quad (17)$$

$\tilde{Z}_{nm}(\tilde{q}_n)$  are the squark wave-function renormalization constants. They stem from gluon, gluino, and squark loops (Figs. 1g–i) and are given by:

$$\delta\tilde{Z}_{nn}^{(g,\tilde{g})}(\tilde{q}_n) = -\text{Re} \left\{ \dot{\Sigma}_{nn}^{(g,\tilde{g})}(m_{\tilde{q}_n}^2) \right\}, \quad \delta\tilde{Z}_{nn'}^{(\tilde{g},\tilde{g})}(\tilde{q}_n) = -\frac{\text{Re} \left\{ \Sigma_{nn'}^{(\tilde{g},\tilde{g})}(m_{\tilde{q}_n}^2) \right\}}{m_{\tilde{q}_n}^2 - m_{\tilde{q}_{n'}}^2}, \quad n \neq n', \quad (18)$$

with  $\dot{\Sigma}_{nn}(m^2) = \partial\Sigma_{nn}(p^2)/\partial p^2|_{p^2=m^2}$ . (The gluon loop due to the  $\tilde{q}\tilde{q}gg$  interaction gives no contribution because it is proportional to the gluon mass  $\lambda \rightarrow 0$ .) The squark self-energy contribution due to gluon exchange (Fig. 1g) is

$$\dot{\Sigma}_{nn}^{(g)}(m_{\tilde{q}_n}^2) = -\frac{2\alpha_s}{3\pi} \left[ B_0(m_{\tilde{q}_n}^2, 0, m_{\tilde{q}_n}^2) + 2m_{\tilde{q}_n}^2 \dot{B}_0(m_{\tilde{q}_n}^2, \lambda^2, m_{\tilde{q}_n}^2) \right], \quad (19)$$

and that due to gluino exchange (Fig. 1h) is

$$\begin{aligned} \dot{\Sigma}_{nn}^{(\tilde{g})}(m_{\tilde{q}_n}^2) &= \frac{2\alpha_s}{3\pi} \left[ B_0(m_{\tilde{q}_n}^2, m_{\tilde{g}}^2, m_q^2) + (m_{\tilde{q}_n}^2 - m_q^2 - m_{\tilde{g}}^2) \dot{B}_0(m_{\tilde{q}_n}^2, m_{\tilde{g}}^2, m_q^2) \right. \\ &\quad \left. - 2m_q m_{\tilde{g}} (-1)^n \sin 2\theta_{\tilde{q}} \dot{B}_0(m_{\tilde{q}_n}^2, m_{\tilde{g}}^2, m_q^2) \right], \end{aligned} \quad (20)$$

$$\Sigma_{12}^{(\tilde{g})}(m_{\tilde{q}_n}^2) = \Sigma_{21}^{(\tilde{g})}(m_{\tilde{q}_n}^2) = \frac{4\alpha_s}{3\pi} m_{\tilde{g}} m_q \cos 2\theta_{\tilde{q}} B_0(m_{\tilde{q}_n}^2, m_{\tilde{g}}^2, m_q^2). \quad (21)$$

The four-squark interaction (Fig. 1i) gives

$$\Sigma_{12}^{(\tilde{q})}(m_{\tilde{q}_n}^2) = \Sigma_{21}^{(\tilde{q})}(m_{\tilde{q}_n}^2) = \frac{\alpha_s}{6\pi} \sin 4\theta_{\tilde{q}} \left[ A_0(m_{\tilde{q}_2}^2) - A_0(m_{\tilde{q}_1}^2) \right], \quad (22)$$

where  $A_0(m^2)$  is the standard one-point function in the convention of [17]. Note that  $\Sigma_{nn'}^{(\tilde{q})}(m_{\tilde{q}_1}^2) = \Sigma_{nn'}^{(\tilde{q})}(m_{\tilde{q}_2}^2)$ .

### 3.3 On-shell renormalization of squark mixing angles

It is necessary to renormalize the squark mixing angles  $\theta_{\tilde{q}}$  by adding appropriate counterterms to obtain ultraviolet finite decay widths:

$$\delta c_{21Z}^{(c)} = -\frac{1}{\cos\theta_W} I_{3L}^q \cos 2\theta_{\tilde{q}} \delta\theta_{\tilde{q}}, \quad (23)$$

$$\begin{aligned} \delta c_{ijW}^{(c)} &= \frac{1}{\sqrt{2}} \left[ \begin{pmatrix} -\sin\theta_{\tilde{q}} \cos\theta_{\tilde{q}'} & \sin\theta_{\tilde{q}} \sin\theta_{\tilde{q}'} \\ -\cos\theta_{\tilde{q}} \cos\theta_{\tilde{q}'} & \cos\theta_{\tilde{q}} \sin\theta_{\tilde{q}'} \end{pmatrix} \delta\theta_{\tilde{q}} \right. \\ &\quad \left. + \begin{pmatrix} -\cos\theta_{\tilde{q}} \sin\theta_{\tilde{q}'} & -\cos\theta_{\tilde{q}} \cos\theta_{\tilde{q}'} \\ \sin\theta_{\tilde{q}} \sin\theta_{\tilde{q}'} & \sin\theta_{\tilde{q}} \cos\theta_{\tilde{q}'} \end{pmatrix} \delta\theta_{\tilde{q}'} \right]_{ij}. \end{aligned} \quad (24)$$

For the definition of the on-shell mixing angles  $\theta_{\tilde{q}}$  we follow the procedure given in Ref. [7]. The counterterm  $\delta\theta_{\tilde{q}}$  is fixed such that it cancels the off-diagonal part of the squark wave function corrections to the cross section of  $e^+e^- \rightarrow \tilde{q}_1\tilde{q}_2$ .  $\delta\theta_{\tilde{q}} = \delta\theta_{\tilde{q}}^{(\tilde{q})} + \delta\theta_{\tilde{q}}^{(\tilde{g})}$  is then given by

$$\delta\theta_{\tilde{q}}^{(\tilde{q})} = \frac{\alpha_s}{6\pi} \frac{\sin 4\theta_{\tilde{q}}}{m_{\tilde{q}_1}^2 - m_{\tilde{q}_2}^2} \left[ A_0(m_{\tilde{q}_2}^2) - A_0(m_{\tilde{q}_1}^2) \right], \quad (25)$$

$$\delta\theta_{\tilde{q}}^{(\tilde{g})} = \frac{\alpha_s}{3\pi} \frac{m_{\tilde{g}}m_q}{I_{3L}^q(m_{\tilde{q}_1}^2 - m_{\tilde{q}_2}^2)} \left[ B_0(m_{\tilde{q}_2}^2, m_{\tilde{g}}^2, m_q^2) \tilde{v}_{11} - B_0(m_{\tilde{q}_1}^2, m_{\tilde{g}}^2, m_q^2) \tilde{v}_{22} \right], \quad (26)$$

with  $\tilde{v}_{11} = 4(I_{3L}^q \cos^2 \theta_{\tilde{q}} - e_q \sin^2 \theta_W)$  and  $\tilde{v}_{22} = 4(I_{3L}^q \sin^2 \theta_{\tilde{q}} - e_q \sin^2 \theta_W)$ . Obviously, for the decay  $\tilde{q}_2 \rightarrow \tilde{q}_1 Z^0$ , the counterterm (23) completely cancels the off-diagonal wave function corrections (Figs. 1h ( $i \neq n$ ) and 1i ( $i \neq k$ )). In case of  $\tilde{q}_i \rightarrow \tilde{q}'_j W^\pm$  the contribution of the squark loop, Fig. 1i, is cancelled. Thus, in both cases the total squark loop contribution to the correction is zero,  $\delta\Gamma^{(\tilde{q})} \equiv 0$ .

### 3.4 Real gluon emission

In order to cancel the infrared divergence we include real (hard and soft) gluon emission:  $\delta\Gamma_{real} = \Gamma(\tilde{q}_i^\alpha \rightarrow \tilde{q}_j^\beta V g)$  (Figs. 1j, 1k, and 1 $\ell$ ). The width is

$$\delta\Gamma_{real} = \frac{g^2 c_{ijV}^2 \alpha_s}{3\pi^2 m_i} \left\{ 2I - \frac{\kappa^2}{m_V^2} \left[ I_0 + I_1 + m_i^2 I_{00} + m_j^2 I_{11} + (m_i^2 + m_j^2 - m_V^2) I_{01} \right] \right\}. \quad (27)$$

Again,  $\kappa = \kappa(m_i^2, m_j^2, m_V^2)$ . The phase space integrals  $I$ ,  $I_n$ , and  $I_{nm}$  have  $(m_i, m_j, m_V)$  as arguments. Their explicit forms are given in [17].

We have checked explicitly that the corrected decay width, eq. (11), is ultraviolet and infrared finite.

## 4 Numerical results and discussion

In general, the stop and sbottom sectors are determined by the soft SUSY breaking parameters ( $M_{\tilde{Q}}$ ,  $M_{\tilde{U}}$ , and  $M_{\tilde{D}}$ ), the trilinear couplings ( $A_t$  and  $A_b$ ),  $\mu$ , and  $\tan\beta$ , which all enter the squark mass matrices. In order to show the importance of the  $\tilde{q}_2 \rightarrow \tilde{q}_1 Z^0$  and  $\tilde{q}_i \rightarrow \tilde{q}'_j W^\pm$  decays, we plot in Fig. 2 the branching ratios of these modes as a function of  $\mu$  for  $M_{\tilde{Q}} = 500$  GeV,  $M_{\tilde{U}} = 444$  GeV,  $M_{\tilde{D}} = 556$  GeV, and  $A_t = A_b = 500$  GeV. For the SU(2) gaugino mass we take

$M = 200$  GeV, and for the mass of the pseudoscalar Higgs  $m_A = 200$  GeV (for the U(1) gaugino mass  $M'$  and the gluino mass we use the GUT relations  $M' = \frac{5}{3} M \tan^2 \theta_W$  and  $m_{\tilde{g}} = \alpha_s/\alpha_2 M$ ). Fig. 2a (2b) is for  $\tan \beta = 2$  (40). We see that the squark decays into vector bosons can have very large branching ratios under the conditions (i), (ii), and (iii) given in the introduction.

We now turn to the numerical analysis of the  $\mathcal{O}(\alpha_s)$  SUSY–QCD corrected decay widths. As the squark couplings to vector bosons depend only on the squark mixing angles, we use the on-shell squark masses  $m_{\tilde{q}_{1,2}}$  and mixing angles  $\theta_{\tilde{q}}$  ( $0 \leq \theta_{\tilde{q}} < \pi$ ) as input parameters. Moreover, we take  $m_t = 175$  GeV,  $m_b = 5$  GeV,  $m_Z = 91.2$  GeV,  $\sin^2 \theta_W = 0.23$ ,  $\alpha(m_Z) = 1/128.87$ , and  $\alpha_s(m_Z) = 0.12$ . For the running of  $\alpha_s$  we use  $\alpha_s(Q^2) = 12\pi/[(33 - 2n_f) \ln(Q^2/\Lambda_{n_f}^2)]$  with  $n_f$  the number of flavors.

We first discuss the decay  $\tilde{t}_2 \rightarrow \tilde{t}_1 Z^0$ . Figure 3 shows the tree–level and the  $\mathcal{O}(\alpha_s)$  SUSY–QCD corrected widths of this decay as a function of the lighter stop mass  $m_{\tilde{t}_1}$ , for  $m_{\tilde{t}_2} = 650$  GeV,  $\cos \theta_{\tilde{t}} = -0.6$ , and  $m_{\tilde{g}} = 500$  GeV. SUSY–QCD corrections reduce the tree–level width by  $-11.7\%$  to  $-6.8\%$  in the range of  $m_{\tilde{t}_1} = 80$  to 508 GeV. It is interesting to note that the gluonic correction decreases quickly with increasing  $m_{\tilde{t}_1}$  while the correction due to gluino exchange varies only little with  $m_{\tilde{t}_1}$ . In our example,  $\delta\Gamma^{(g)}/\Gamma^0 = -4.5\%$  and  $\delta\Gamma^{(\tilde{g})}/\Gamma^0 = -7.2\%$  at  $m_{\tilde{t}_1} = 80$  GeV, whereas at  $m_{\tilde{t}_1} = 550$  GeV  $\delta\Gamma^{(g)}/\Gamma^0 \simeq 0\%$  and  $\delta\Gamma^{(\tilde{g})}/\Gamma^0 = -6.8\%$ .

The dependence on the stop mixing angle is shown in Fig. 4. Fig. 4a shows the tree–level width together with the  $\mathcal{O}(\alpha_s)$  corrected width of  $\tilde{t}_2 \rightarrow \tilde{t}_1 Z^0$  as a function of  $\cos \theta_{\tilde{t}}$  for  $m_{\tilde{t}_1} = 200$  GeV,  $m_{\tilde{t}_2} = 650$  GeV, and  $m_{\tilde{g}} = 500$  GeV. Assuming  $M_{\tilde{U}} < M_{\tilde{Q}}$ , as suggested by SUSY–GUT, the stop mixing angle is varied in the range  $-\frac{1}{\sqrt{2}} < \cos \theta_{\tilde{t}} < \frac{1}{\sqrt{2}}$ . With the  $\tilde{t}_1$ – $\tilde{t}_2$ – $Z^0$  coupling proportional to  $\sin 2\theta_{\tilde{t}}$  the decay width has maxima at  $\cos \theta_{\tilde{t}} = \pm \frac{1}{\sqrt{2}}$  (maximal mixing) and vanishes at  $\cos \theta_{\tilde{t}} = 0$ . In Fig. 4b we plot the relative correction  $\delta\Gamma/\Gamma^0$  for  $m_{\tilde{t}_{\{1,2\}}} = \{200, 650\}$  GeV and  $m_{\tilde{g}} = 500$  and 1000 GeV. As the gluonic correction has the same  $\theta_{\tilde{t}}$  dependence as the tree–level width,  $\delta\Gamma^{(g)}/\Gamma^0 = -3\%$  in our example, the  $\theta_{\tilde{t}}$  dependence in Fig. 4b comes only from the correction due to gluino exchange. For  $m_{\tilde{g}} = 500$  GeV and  $\cos \theta_{\tilde{t}} \lesssim -0.1$  ( $\cos \theta_{\tilde{t}} \gtrsim 0.1$ ) the correction is  $-10\%$  to  $-12\%$  ( $-3\%$  to  $-5\%$ ); for  $m_{\tilde{g}} = 1$  TeV and  $|\cos \theta_{\tilde{t}}| \gtrsim 0.1$  the correction is  $-2\%$  to  $-5\%$ . Approaching  $\cos \theta_{\tilde{t}} = 0$ , where  $\tilde{t}_{1(2)} = \tilde{t}_{R(L)}$ ,  $\delta\Gamma/\Gamma^0$  diverges due to the vanishing tree–level coupling  $c_{21Z}$  while  $\delta c_{21Z} \neq 0$ . In this case the decay width becomes of  $\mathcal{O}(\alpha_s^2)$ . Note, however, that the appearance of this divergence, as well as the condition  $\cos \theta_{\tilde{t}} = 0$ , is renormalization scheme dependent.

Taking a closer look on the gluino mass dependence we find that the gluino decouples slowly; e.g. for  $m_{\tilde{t}_1} = 200$  GeV,  $m_{\tilde{t}_2} = 650$  GeV, and  $\cos \theta_{\tilde{t}} = -0.6$  the gluino contribution to the correction  $\delta\Gamma^{(\tilde{g})}/\Gamma^0 = -2.6\%$ ,  $-0.8\%$ ,  $-0.4\%$  for  $m_{\tilde{g}} = 600$  GeV, 1 TeV, 1.5 TeV, respectively. On the

other hand, the size of the gluino contribution quickly increases when approaching the  $\tilde{t}_2 \rightarrow t\tilde{g}$  threshold: For  $m_{\tilde{g}} = 480$  GeV  $\delta\Gamma^{(\tilde{g})}/\Gamma^0 = -17.2\%$ , and for  $m_{\tilde{g}} = 476$  GeV  $\delta\Gamma^{(\tilde{g})}/\Gamma^0 = -38.8\%$ . For  $m_{\tilde{g}} < m_{\tilde{t}_2} - m_t$  the gluino correction becomes positive. In our example it reaches the maximum at  $m_{\tilde{g}} = 270$  GeV with  $\delta\Gamma^{(\tilde{g})}/\Gamma^0 = 3.4\%$ . In general, the dependence on the gluino mass near the threshold is less pronounced for  $\cos\theta_{\tilde{t}} > 0$ .

The decay  $\tilde{b}_2 \rightarrow \tilde{b}_1 Z^0$  can be important for large  $\tan\beta$  (see Fig. 2b). The SUSY–QCD corrections to this decay behave similarly to those to  $\tilde{t}_2 \rightarrow \tilde{t}_1 Z^0$ . However, the corrections due to gluino exchange are smaller because of the smaller bottom quark mass and thus the dependence of  $\delta\Gamma/\Gamma^0$  on the sbottom mixing angle is very weak.

Let us now turn to the squark decays into  $W^\pm$  bosons. Here we discuss two special cases:

- (i)  $\tilde{b}_1$  and  $\tilde{b}_2$  decaying into a relatively light  $\tilde{t}_1$  plus  $W^-$  for small sbottom mixing (small  $\tan\beta$  scenario). In this case the mass difference of  $\tilde{b}_1$  and  $\tilde{b}_2$  is expected to be rather small and thus the decays  $\tilde{b}_2 \rightarrow \tilde{b}_1 (Z^0, h^0, H^0, A^0)$  should be kinematically suppressed or even forbidden.
- (ii) A heavy  $\tilde{t}_2$  decaying into a relatively light  $\tilde{b}_1$  plus  $W^+$  for large sbottom mixing (large  $\tan\beta$  scenario).

Note, however, that in a combined treatment of both the stop and the sbottom sectors there is a constraint among the parameters  $m_{\tilde{t}_1}$ ,  $m_{\tilde{t}_2}$ ,  $\theta_{\tilde{t}}$ ,  $m_{\tilde{b}_1}$ ,  $m_{\tilde{b}_2}$ , and  $\theta_{\tilde{b}}$  (for a given value of  $\tan\beta$ ) due to  $SU(2)_L$  gauge symmetry [10, 18]. Therefore one of these parameters is fixed by the others. Here one has to take into account that in the on-shell scheme  $M_Q^2(\tilde{t}) \neq M_Q^2(\tilde{b})$  at  $\mathcal{O}(\alpha_s)$ , see Ref. [18].

The decay widths of  $\tilde{b}_{1,2} \rightarrow \tilde{t}_1 W^-$  are shown in Fig. 5a as a function of the stop mixing angle, for  $m_{\tilde{b}_1} = 500$  GeV,  $m_{\tilde{b}_2} = 520$  GeV,  $\cos\theta_{\tilde{b}} = -0.9$ ,  $m_{\tilde{t}_1} = 200$  GeV,  $m_{\tilde{g}} = 520$  GeV, and  $\tan\beta = 2$ . The value of  $m_{\tilde{t}_2}$  is determined by the other parameters as discussed above. Hence  $m_{\tilde{t}_2}$  varies from 533 GeV to 733 GeV depending on the stop mixing angle in Fig. 5a. (Here we have also checked that the squark parameters do not cause too large  $A_t$  or  $A_b$  to avoid color breaking minima.) Despite the larger phase space for the  $\tilde{b}_2$  decay, the width of  $\tilde{b}_2 \rightarrow \tilde{t}_1 W^-$  is smaller than that of  $\tilde{b}_1 \rightarrow \tilde{t}_1 W^-$  because the  $W$  couples only to the “left” components of the squarks (note that  $\tilde{b}_1 \sim \tilde{b}_L$  and  $\tilde{b}_2 \sim \tilde{b}_R$  for  $\cos\theta_{\tilde{b}} = -0.9$ ). Fig. 5b shows the relative correction  $\delta\Gamma/\Gamma^0$  for the same squark parameters as in Fig. 5a. For  $m_{\tilde{g}} = 520$  GeV and  $|\cos\theta_{\tilde{t}}| \gtrsim 0.1$  SUSY–QCD corrections are  $-11\%$  to  $+4\%$ . For  $m_{\tilde{g}} = 1$  TeV the effects are weaker, i.e. about  $-5\%$  to  $-1\%$ . Again, there is a “singularity” at  $\cos\theta_{\tilde{t}} = 0$  where the tree-level  $\tilde{t}_1$ - $\tilde{b}_i$ - $W^\pm$  coupling vanishes. The dependence of  $\delta\Gamma/\Gamma^0$  on the sbottom mixing angle is, in general, much weaker than that on the stop mixing angle (apart from a singularity for the  $\tilde{b}_i$  being a pure  $\tilde{b}_R$ ). The overall dependence on the gluino mass is in general similar to that of the  $\tilde{t}_2 \rightarrow \tilde{t}_1 Z^0$  decay. However,

the enhancement effect of the threshold at  $m_{\tilde{g}} = m_{\tilde{b}_i} - m_b$  is less pronounced.

An example for large  $\tan \beta$  is shown in Fig. 6. In Fig. 6a we plot the tree-level and the SUSY–QCD corrected widths of  $\tilde{t}_2 \rightarrow \tilde{b}_1 W^+$  as a function of  $\cos \theta_{\tilde{t}}$  for  $m_{\tilde{t}_1} = 300 \text{ GeV}$ ,  $m_{\tilde{t}_2} = 650 \text{ GeV}$ ,  $m_{\tilde{b}_1} = 380 \text{ GeV}$ ,  $\cos \theta_{\tilde{b}} = -0.8$ ,  $m_{\tilde{g}} = 500 \text{ GeV}$ , and  $\tan \beta = 40$ .  $m_{\tilde{b}_2}$  is calculated from the other parameters and thus varies from 615 GeV to 918 GeV. As expected, the decay width is maximal for  $\tilde{t}_2 = \tilde{t}_L$  and vanishes for  $\tilde{t}_2 = \tilde{t}_R$ . In the example chosen, SUSY–QCD corrections are  $-2.4\%$  to  $-4.7\%$  for  $m_{\tilde{g}} = 500 \text{ GeV}$  and about  $-1\%$  to  $-1.5\%$  for  $m_{\tilde{g}} = 1 \text{ TeV}$  as can be seen in Fig. 6b, where  $\delta\Gamma/\Gamma^0$  is shown as a function of  $\cos \theta_{\tilde{t}}$  for the same squark parameters as given above, and  $m_{\tilde{g}} = 500 \text{ GeV}$  and  $1 \text{ TeV}$ . Again, there is almost no dependence on  $\cos \theta_{\tilde{b}}$  apart from the singularity at  $\cos \theta_{\tilde{b}} = 0$ , i.e.  $\tilde{b}_1 = \tilde{b}_R$ .

## 5 Summary

We have calculated the  $\mathcal{O}(\alpha_s)$  supersymmetric QCD corrections to squark decays into vector bosons in the on-shell renormalization scheme using dimensional reduction. In particular, we have discussed examples for the decays  $\tilde{t}_2 \rightarrow \tilde{t}_1 Z^0$ ,  $\tilde{t}_2 \rightarrow \tilde{b}_1 W^+$ , and  $\tilde{b}_{1,2} \rightarrow \tilde{t}_1 W^-$ . We have found that the correction  $\delta\Gamma/\Gamma^0$  is typically of the order  $-5\%$  to  $-10\%$ , depending on the squark masses, squark mixing angles, and  $m_{\tilde{g}}$ . Near the  $\tilde{q} \rightarrow q\tilde{g}$  threshold the correction can also exceed  $-10\%$ . It has also turned out that the gluino decouples slowly. Moreover, the gluino–exchange corrections alter the  $\theta_{\tilde{q}}$  dependence of the tree-level widths. For squark mixing angles where the decay width vanishes at tree-level, the gluino corrections do not vanish and may lead to non-zero widths of  $\mathcal{O}(\alpha_s^2)$ .

## Acknowledgements

The work of A.B., H.E., S.K., W.M., and W.P. was supported by the “Fonds zur Förderung der wissenschaftlichen Forschung” of Austria, project no. P10843–PHY.

## References

- [1] For a review, see:  
H. P. Nilles, Phys. Rep. 110 (1984) 1;  
H.E. Haber, G.L. Kane, Phys. Rep. 117 (1985) 75;  
R. Barbieri, Riv. Nuov. Cim. 11 (1988) 1.
- [2] J. Ellis, S. Rudaz, Phys. Lett. B128 (1983) 248;  
J.F. Gunion, H.E. Haber, Nucl. Phys. B272 (1986) 1; B402 (1993) 567 (E).
- [3] K. Hikasa, M. Kobayashi, Phys. Rev. D36 (1987) 724.
- [4] M. Drees, K. Hikasa, Phys. Lett. B252 (1990) 127.
- [5] W. Beenakker, R. Höpker, P. M. Zerwas, Phys. Lett. B349 (1995) 463.
- [6] A. Arhrib, M. Capdequi-Peyranere, A. Djouadi, Phys. Rev. D52 (1995) 1404.
- [7] H. Eberl, A. Bartl, W. Majerotto, Nucl. Phys. B472 (1996) 481.
- [8] W. Beenakker, R. Höpker, M. Spira, P. M. Zerwas, Nucl. Phys. B492 (1997) 51.
- [9] A. Bartl, W. Majerotto, W. Porod, Z. Phys. C 64 (1994) 499; C 68 (1995) 518 (E).
- [10] A. Bartl, H. Eberl, S. Kraml, W. Majerotto, W. Porod, A. Sopczak, hep-ph/9701336, to appear in Z. Phys. C.
- [11] ECFA/DESY LC Physics Working Group: E. Accomando, et al., DESY 97-100, hep-ph/9705442, to be published in Phys. Rep.;  
A. Bartl, H. Eberl, T. Gajdosik, S. Kraml, W. Majerotto, W. Porod, A. Sopczak, hep-ph/9709252, contribution to the proceedings “ECFA/DESY Study on Physics and Detectors for the Linear Collider”, DESY 97-123E, ed. R. Settles.
- [12] S. Kraml, H. Eberl, A. Bartl, W. Majerotto, W. Porod, Phys. Lett. B386 (1996) 175;  
A. Djouadi, W. Hollik, C. Jünger, Phys. Rev. D55 (1997) 6975.
- [13] A. Arhrib, A. Djouadi, W. Hollik, C. Jünger, hep-ph/9702426.
- [14] W. Beenakker, R. Höpker, P. M. Zerwas, Phys. Lett. B378 (1996) 159;  
W. Beenakker, R. Höpker, T. Plehn, P. M. Zerwas, Z. Phys. C 75 (1997) 349.
- [15] W. Siegel, Phys. Lett. B84 (1979) 193;  
D. M. Capper, D. R. T. Jones, P. van Nieuwenhuizen, Nucl. Phys. B167 (1980) 479;  
I. Jack, D. R. T. Jones, hep-ph/9707278.
- [16] G. Passarino, M. Veltman, Nucl. Phys. B160 (1979) 151.
- [17] A. Denner, Fortschr. Phys. 41 (1993) 307.

[18] A. Bartl, H. Eberl, K. Hidaka, T. Kon, W. Majerotto, Y. Yamada, Phys. Lett. B402 (1997) 303.

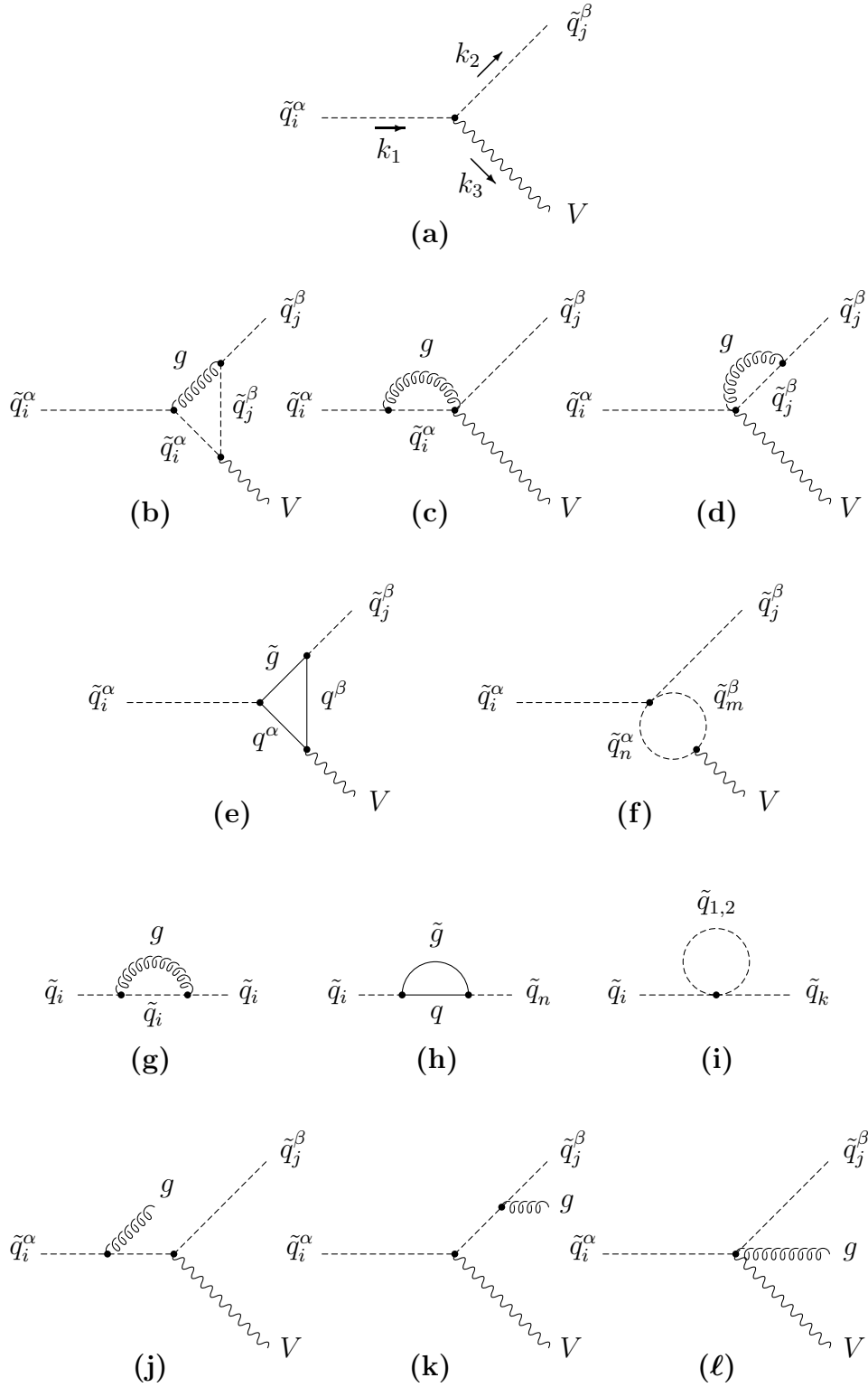


**Fig. 1:** Feynman diagrams relevant for the  $\mathcal{O}(\alpha_s)$  SUSY-QCD corrections to squark decays into vector bosons.

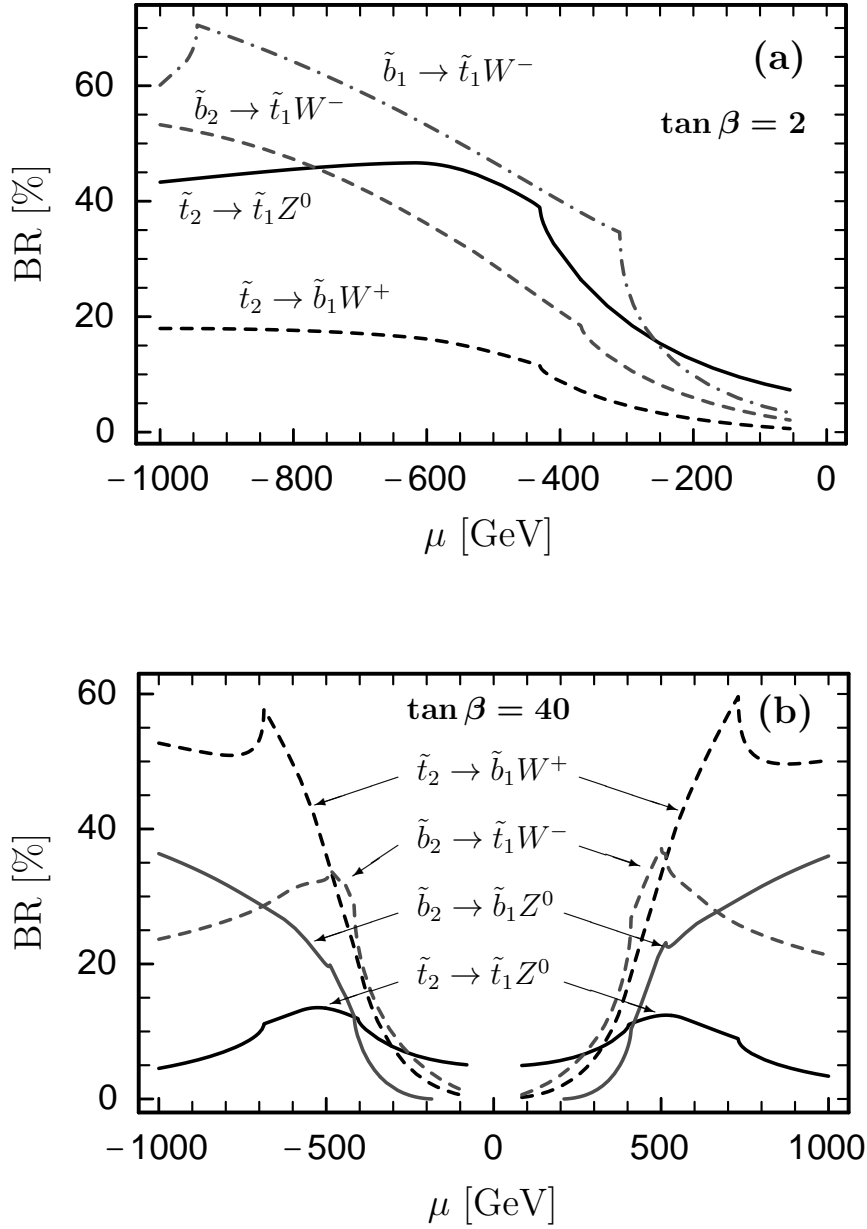


**Fig. 2:** Tree-level branching ratios for stop and sbottom decays into vector bosons as a function of  $\mu$ , for  $M_{\tilde{Q}} = 500$  GeV,  $M_{\tilde{U}} = 444$  GeV,  $M_{\tilde{D}} = 556$  GeV,  $A_t = A_b = 500$  GeV,  $M = 200$  GeV, and  $m_A = 200$  GeV. **(a)**  $\tan \beta = 2$ , and **(b)**  $\tan \beta = 40$ .

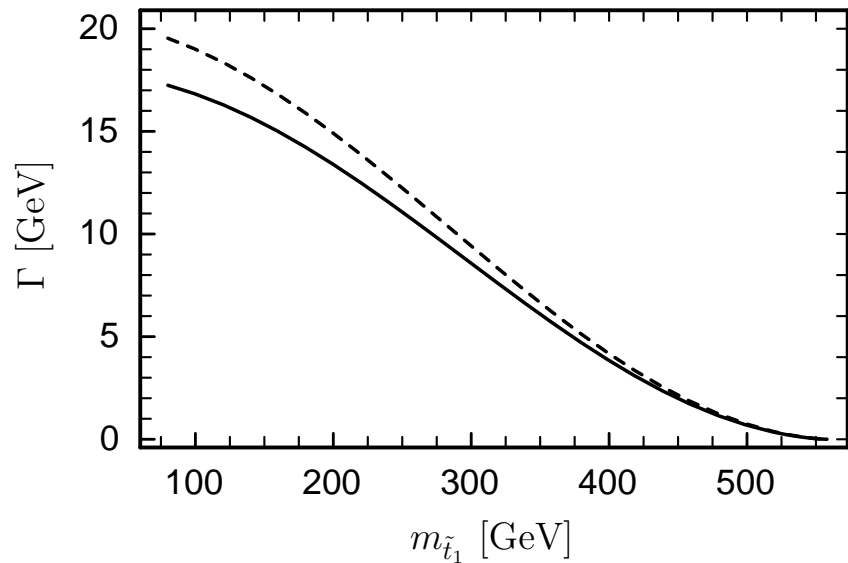


**Fig. 3:** Tree-level (dashed line) and SUSY-QCD corrected (solid line) widths of the decay  $\tilde{t}_2 \rightarrow \tilde{t}_1 Z^0$  as a function of  $m_{\tilde{t}_1}$  for  $m_{\tilde{t}_2} = 650$  GeV,  $\cos \theta_{\tilde{t}} = -0.6$ , and  $m_{\tilde{g}} = 500$  GeV.

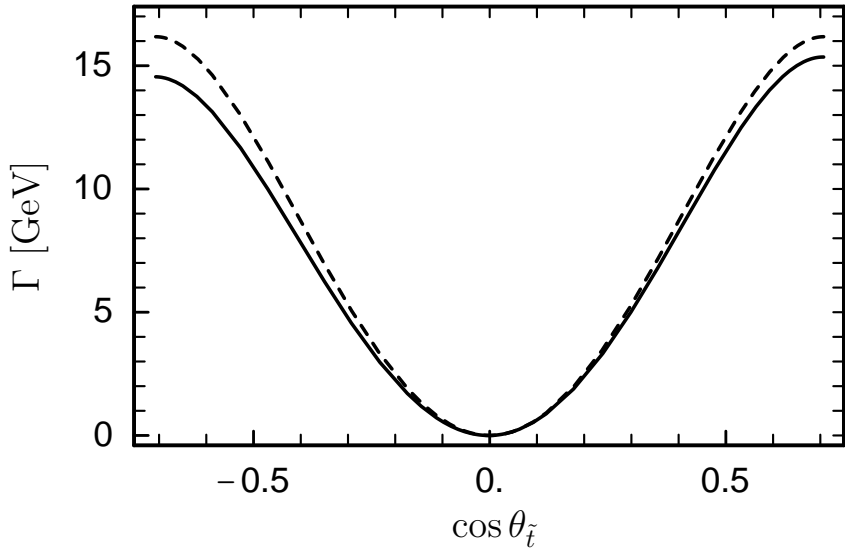


**Fig. 4a:** Tree-level (dashed line) and SUSY-QCD corrected (solid line) widths of the decay  $\tilde{t}_2 \rightarrow \tilde{t}_1 Z^0$  as a function of  $\cos \theta_{\tilde{t}}$  for  $m_{\tilde{t}_1} = 200$  GeV,  $m_{\tilde{t}_2} = 650$  GeV, and  $m_{\tilde{g}} = 500$  GeV.

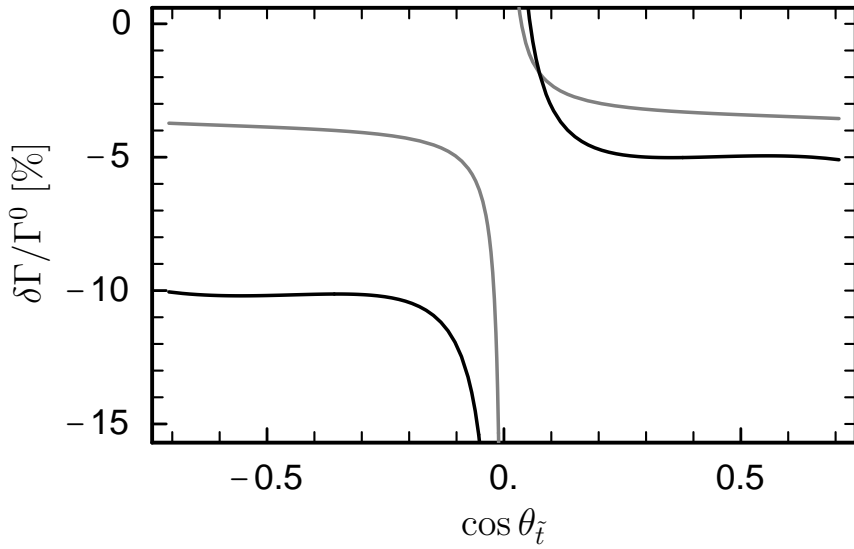


**Fig. 4b:** SUSY-QCD correction relative to the tree-level width of the decay  $\tilde{t}_2 \rightarrow \tilde{t}_1 Z^0$  as a function of  $\cos \theta_{\tilde{t}}$  for  $m_{\tilde{t}_1} = 200$  GeV and  $m_{\tilde{t}_2} = 650$  GeV. The black (gray) lines are for  $m_{\tilde{g}} = 500$  (1000) GeV.

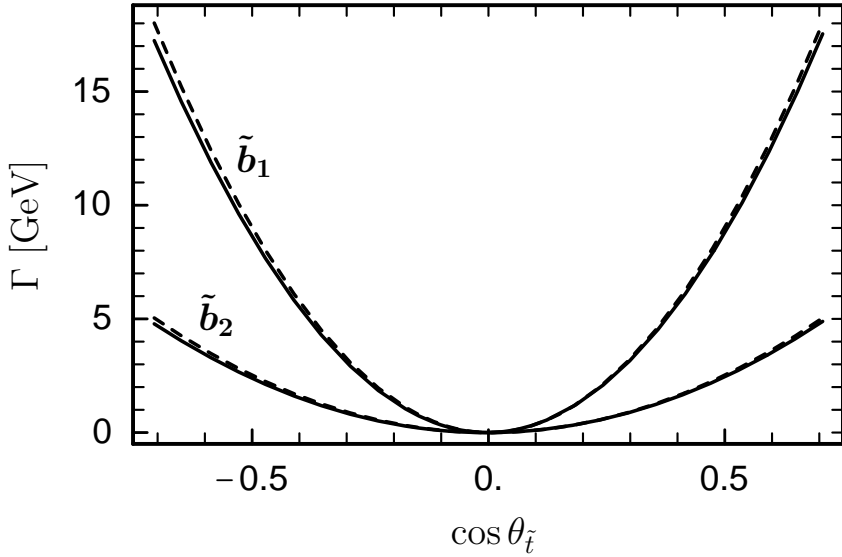


**Fig. 5a:** Tree-level (dashed lines) and SUSY-QCD corrected (solid lines) widths of the decays  $\tilde{b}_{1,2} \rightarrow \tilde{t}_1 W^-$  as a function of  $\cos \theta_{\tilde{t}}$  for  $m_{\tilde{b}_1} = 500$  GeV,  $m_{\tilde{b}_2} = 520$  GeV,  $\cos \theta_{\tilde{b}} = -0.9$ ,  $m_{\tilde{t}_1} = 200$  GeV,  $m_{\tilde{g}} = 520$  GeV, and  $\tan \beta = 2$ .  $m_{\tilde{t}_2}$  is a function of the other parameters and varies with  $\cos \theta_{\tilde{t}}$ .

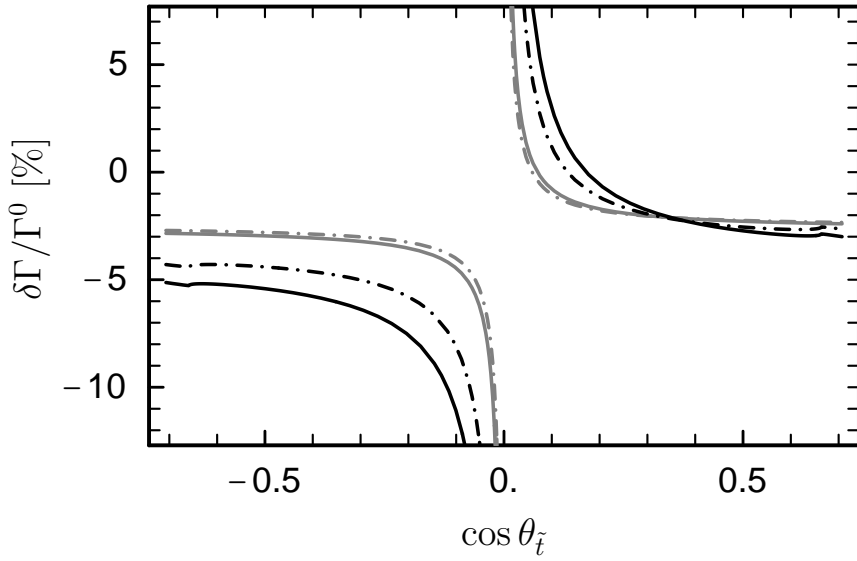


**Fig. 5b:** SUSY-QCD corrections relative to the tree-level widths of the decays  $\tilde{b}_1 \rightarrow \tilde{t}_1 W^-$  (dashdotted lines) and  $\tilde{b}_2 \rightarrow \tilde{t}_1 W^-$  (solid lines) as a function of  $\cos \theta_{\tilde{t}}$  for  $m_{\tilde{b}_1} = 500$  GeV,  $m_{\tilde{b}_2} = 520$  GeV,  $\cos \theta_{\tilde{b}} = -0.9$ ,  $m_{\tilde{t}_1} = 200$  GeV, and  $\tan \beta = 2$ . The black (gray) lines are for  $m_{\tilde{g}} = 520$  (1000) GeV.  $m_{\tilde{t}_2}$  is a function of the other parameters, as in Fig. 5a.

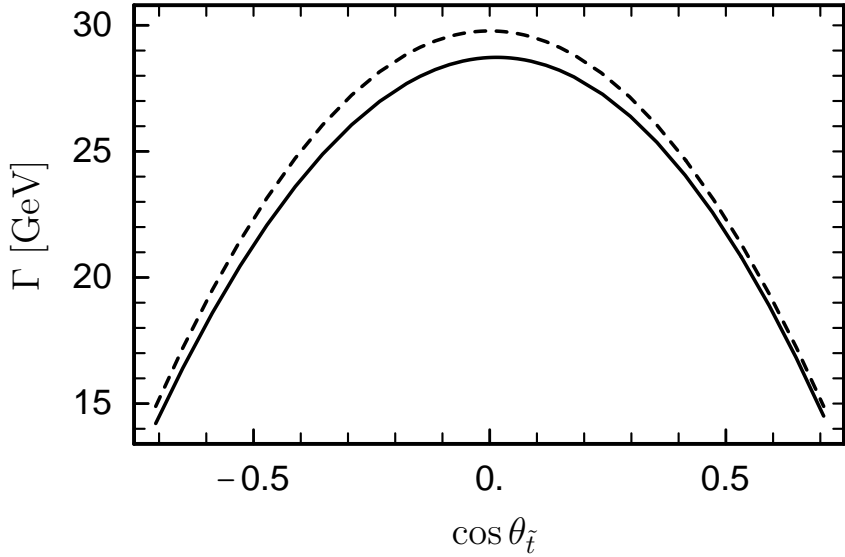


**Fig. 6a:** Tree-level (dashed line) and SUSY-QCD corrected (solid line) widths of the decay  $\tilde{t}_2 \rightarrow \tilde{b}_1 W^+$  as a function of  $\cos \theta_{\tilde{t}}$  for  $m_{\tilde{t}_1} = 300$  GeV,  $m_{\tilde{t}_2} = 650$  GeV,  $m_{\tilde{b}_1} = 380$  GeV,  $\cos \theta_{\tilde{b}} = -0.8$ ,  $m_{\tilde{g}} = 500$  GeV, and  $\tan \beta = 40$ .  $m_{\tilde{b}_2}$  is a function of the other parameters and varies with  $\cos \theta_{\tilde{t}}$ .

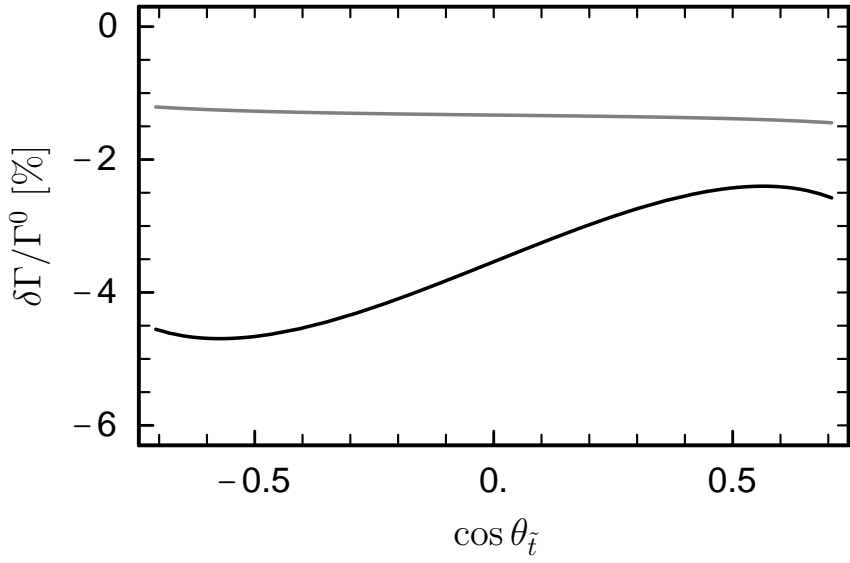


**Fig. 6b:** SUSY-QCD corrections relative to the tree-level width of the decay  $\tilde{t}_2 \rightarrow \tilde{b}_1 W^+$  as a function of  $\cos \theta_{\tilde{t}}$  for  $m_{\tilde{t}_1} = 300$  GeV,  $m_{\tilde{t}_2} = 650$  GeV,  $m_{\tilde{b}_1} = 380$  GeV,  $\cos \theta_{\tilde{b}} = -0.8$ , and  $\tan \beta = 40$ . The black (gray) line is for  $m_{\tilde{g}} = 500$  (1000) GeV.  $m_{\tilde{b}_2}$  is a function of the other parameters, as in Fig. 6a.